INVESTIGATING THE ROLE OF REFLECTED ELECTRONS IN MULTIPACTOR BREAKDOWN FOR TE_{10} MODE CONFIGURED RECTANGULAR WAVEGUIDES

Akoma Henry E.C.A[1], Adediran Y.A[2]
[1]National Space Research and Development Agency (NASRDA), Abuja, Nigeria
[2]University of Ilorin, Kwara State, Nigeria

ABSTRACT

Reflected electrons are often unaccounted for in multipactor (MP) prediction algorithms supposedly because of how little they contribute to the initiation of multipaction. This research work investigated this claim by comparing the enhanced counter function values of simulation scenarios that included reflection electrons and those that did not, for a range of transmit power levels, in a space-borne rectangular waveguide with TE_{10} propagation mode using a developed MP prediction algorithm. Results generated indicated that, in the case were reflected electrons were properly accounted for, there were more transmit power levels with larger values of enhanced counter function (or increased electron population) than the case where consideration was not given to reflected electrons. The result also indicated that a multipactor discharge event can occur where under some current techniques multipactor is predicted not to occur.

KEYWORDS: *multipactor breakdown, multipactor prediction, secondary emission, reflected electrons, rectangular waveguide.*

I. INTRODUCTION

Conventional multipactor suppression techniques such as surface treatments require that a good percentage of the inner surface of the geometry of interest be coated or sputtered with a material with low secondary electron yield. Similarly, surface geometry modification techniques may require that the geometry surface modification be extensive. Given the risk of placing MP suppressive magnetic fields close to satellite-borne equipment, full surface coating and centre-line grooving of waveguide have received support as acceptable suppression techniques [1][2]. The challenge here is that the center-line may not be the optimum emission point of multipactor-initiating electrons and also applying full coating on the metal surface may just be financially wasteful as only the portion of the waveguide surface emitting the multipactor-initiating electrons need be coated. Understanding this limitation and others, the European Space Agency (ESA) awarded a contract titled "Multipactor and Corona Discharge: Simulation and Design in Microwave Components", which was devoted essentially to the investigation of multipactor and corona effects in rectangular waveguide components through the development of multipactor prediction software tools. The multipactor predictor was required to possess the capability, not only to analyze the electromagnetic response of microwave components but also to determine (predict) the breakdown power of such structures with reasonable accuracy [3]. In essence, this incorporated multipactor prediction into the design and manufacturing process of RF and microwave hardware.

Unfortunately however, some works on multipaction prediction account only for true secondary electrons while completely neglecting the reflected electrons. This is because, many researchers believe that reflected primary electrons play no direct role in electron multiplication between two

surfaces, hence, can be ignored for multipactor discharges under vacuum conditions [3][4]. Reference [5] demonstrated however that the inclusion of electron reflected from the surfaces of vacuum electronic systems predicts the occurrence of multipactor where it would not otherwise occur. Works by [6] and [7] have also shown the relevance of including reflection electrons in multipacting analysis. The former stated clearly that it is a noticeable phenomenon in multipaction testing which has been revealed by empirical current measurement during breakdown and the latter explicitly employed the Furman secondary emission model [8] which fully accounts for reflected electrons. In line with the ESA contract award, this research paper presents a multipactor prediction algorithm capable of predicting possible multipactor initiating RF power levels and optimizing current suppression techniques. The key emphasis of the research was to determine what effect the inclusion or non-inclusion of reflected electrons into the MP prediction algorithm will have on the multipacting process in a typical rectangular waveguide geometry configured for a TE_{10} propagation mode.

The rest of the manuscript is organized as follows: Section 2 itemizes the considerations and assumptions guiding the development of the MP prediction algorithm used for the simulation, and then details the development process itself taking each stage of the multipacting process and the models employed for those stages. Section 3 gives explanations of the algorithm implementation and validation processes. Section 4 presents the results and discussion on them. Finally, section 5 provides the conclusion to the work.

II. THE MULTIPACTOR PREDICTION ALGORITHM

Design Considerations and Assumptions

As indicated earlier, the key emphasis of this research was to determine what effect the inclusion or non-inclusion of reflected electrons in the MP prediction algorithm will have on the multipacting process in a typical rectangular waveguide geometry configured for a TE_{10} mode. Hence, the design process for the presented algorithm hinges on a proper account and consideration for all the various types of electron "emissions" that are probable during a multipacting process - true secondaries and reflected electrons.

A few of the assumptions guiding the development of the algorithm included the following: all the primary electrons were created during the first period of the electromagnetic (EM) field; the initial primary electron population size was a minimum of 1000 electrons; emitted primary electrons possessed non-zero energy levels; since only the onset of the multipactor discharge is to be predicted, electron dynamics were influenced only by the EM field but not affected by the presence of other electrons (space charge); the collision of an electron with a plate could rip zero (absorption), one, or more electrons from the wall and the total kinetic energy of the emitted electron(s) is equal to or less than the kinetic energy of the impacting electron.

The MP Prediction Algorithm

The MP process begins with the generation of primary electrons from the bottom plate of the rectangular waveguide during the first period of the EM field following a uniform distribution. Each electron is emitted with an energy distribution of 2 eV at a velocity perpendicular to the emission surface. A few predictor algorithms have used external EM solvers to obtain the field map for the structure of interest [6] [9]. In contrast, the algorithm in this article incorporates the EM field solver. The EM field distribution for a rectangular waveguide structure with TE_{10} dominant mode was computed using the equations

$$E_y = E_0 \sin\frac{\pi x}{a}\cos(\omega t - \beta z) \quad (1)$$

$$H_x = -\frac{E_0}{Z_{TE}}\sin\frac{\pi x}{a}\cos(\omega t - \beta z) \quad (2)$$

$$H_z = \frac{jE_0}{\eta}\left(\frac{\lambda}{2a}\right)\cos\frac{\pi x}{a}\cos(\omega t - \beta z) \quad (3)$$

Fig. 1 shows a typical TE_{10} mode configured rectangular waveguide, indicating also the directions of the electric field, magnetic field and EM wave propagation.

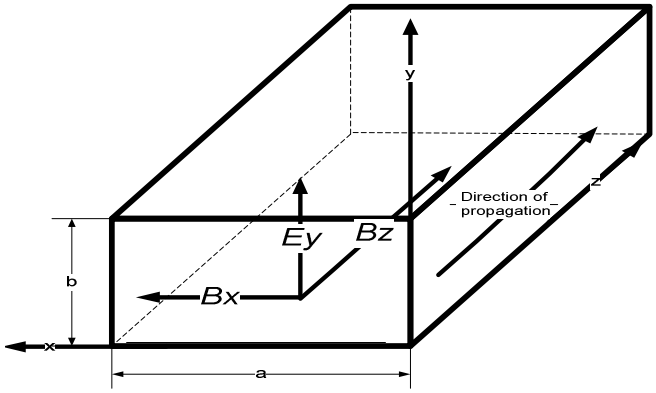

Fig. 1 TE_{10} mode EM field configurations in a rectangular waveguide indicating the directions of the electric field, magnetic field and EM wave propagation

To compute and analyze the electron trajectory, the 4th Order Runge Kutta method was used to solve the non-relativistic Lorentz force equation which is expressed as

$$\boldsymbol{F} = m_e \frac{d\boldsymbol{v}}{dt} = -e(\boldsymbol{E} + \boldsymbol{v} \times \boldsymbol{B}) \tag{4}$$

$$\begin{cases} \frac{d\boldsymbol{v}}{dt} = \frac{-e}{m_e}(\boldsymbol{E} + \boldsymbol{v} \times \boldsymbol{B}) \\ \boldsymbol{v} = \frac{d\boldsymbol{R}}{dt} \end{cases} \tag{5}$$

Fig. 2 shows the trajectory of an electron just before impact with a wall surface. The pre-impact position, *k*, is given as (X_{p-1}, Y_{p-1}, Z_{p-1}) and the impact position, *f*, is given as (X_p, Y_p, Z_p). The electron trajectory is both vertical and horizontal. The vertical distance covered from the pre-impact position to the impact position is the change in *y*-coordinate. The difference between the *y* coordinates is extremely small and so may be assumed to be a straight line. Therefore, the angle of impact, *Φi*, is computed as

$$\Phi_i = \tan\left[\frac{hypot(X_p - X_{p-1}, Z_p - Z_{p-1})}{Y_p - Y_{p-1}}\right] \tag{6}$$

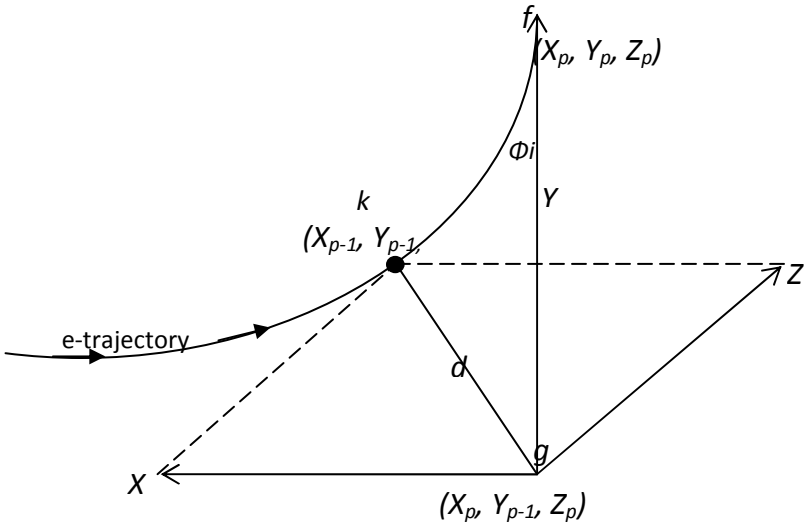

Fig. 2 Determination of angle of impact *Φi*

To compute the total secondary electron yield (SEY), this work combined the Geng SEY model [10] shown in eqn. (7) with Poisson distribution in order to determine the proper average number of true secondary electrons generated per impacting electron. This modified approach is preferred because due consideration is given to the probability that a collision does produce true secondary electrons and also the probability for this collision to produce a certain number of true secondary electrons.

$$\delta(u) = \delta_m \left(\frac{1-\exp\left[-\mathrm{A}(\mathrm{u}/u_m)^{\mathrm{B}}\right]}{C(\mathrm{u}/u_m)^D} \right) \quad (7)$$

Parameter u is the impacting energy (eV) of the primary electron, δ_m is the maximum SEY corresponding to an impacting energy of u_m and the curved fitted *ABCD* parameters are A = 1.55, B = 0.9, C = 0.79, and D = 0.35. In addition, the modified Geng model is combined with a secondary emission probability distribution proposed by [11] in order to properly account for reflected (elastic and inelastic) electrons in the multipacting process. Both elastic and inelastic collisions produce one emitted electron. In the first case, the incoming electron is perfectly reflected. In the second case, the electron penetrates into the material, scattering one electron from atoms inside the material, which is eventually reflected out with energy loss.

Because the emissions considered in this work take consideration of true secondary and reflected electrons, different models were used for computing their emission energy distributions by making use of the principles of conservation of energy and material work function. The distribution of the true secondary electron emission energies is largely independent of the primary electron energy [3] [5]. The first of the n secondaries is assigned the maximum possible energy [4]. Thus,

$$E_{s,max} = \frac{wkfn}{3} \quad (8)$$

The energy levels of the other electrons are computed from the expression

$$E_s(next) = E_s(previous) - E_s(previous) * random\ value \quad (9)$$

where parameter E_s is the emission energy of the secondary electron and $wkfn$ is the work function of the coating material on the wall surface. The *random value* is generated using a Gaussian probability distribution. The elastically reflected secondary electron retains the same energy as that of the primary electron that generated it. Thus,

$$E_s = E_p \quad (10)$$

An inelastic collision with a wall surface result in a percentage of the impact electron energy being transferred (lost) to the impacted atom [5]. Because the atom is massive with respect to the electron, it barely recoils and the electron reflects with a velocity nearly equal in magnitude to its incident velocity. The transferred energy is a function of the ratio of the masses of the electron and impacted atom as well as the velocity of the impacting electron [12] [13]. This is given as

$$E_{transferred}(eV) = \left(4 * \left(\frac{m_e}{m_{atom}}\right) * \frac{1}{2} m_e {v_e}^2\right)/e \quad (11)$$

Hence, on reflected, the energy of the secondary electron is computed as:

$$E_s = E_{impact} - E_{transferred} \quad (12)$$

This model provides a better approach to determining the emission energy of an in-elastically reflected electron when compared to other approaches offered by some researchers which neither takes into consideration the ratio of masses of the electron and the impacted atom nor the velocity of the impacting electron.

III. THE ALGORITHM CODE IMPLEMENTATION

The simulation code was implemented using the MATLAB software. Electron gap crossings were limited to 10-gap crossings, given the limited computational resource. In spite of this limited number of crossings implemented, the quantity of emitted virtual electrons was so large at certain power levels that the computer memory could no longer handle the computation involved. Consequently, the computer system would display an "inadequate memory" error message and then stall further computation. Under this circumstance it was difficult to predict what the quantity of emitted virtual secondary electrons would be at the 10^{th} iteration. To overcome this particular challenge, an extrapolation technique was applied to enable the determination of what could be the possible

population size of the emitted virtual electrons at the end of the 10th iteration. The extrapolation technique employed used a growth function which uses existing data to calculate predicted exponential growth. The growth function was preferred to other extrapolation function types, such as forecast function, trend function, linest function, logest function and slope function because, similar to the growth of emitted electrons, its implementation used an exponential model. MS Excel Spreadsheet has an implementation of this function and so was used for the extrapolation process.

Validation

The result obtained by [10] during an experimental research on MP prediction and suppression on a niobium (*Nb*) coated rectangular waveguide surface is shown in fig. 3. The result shows the values of the normalized enhanced counter function (*Nen*) for power levels from 0 kW to 500 kW at 500 MHz operating frequency for a TE_{10} transverse wave mode at maximum 20-gap crossings. The results so generated by the proposed MP prediction algorithm in this work were compared with those obtained by [10] for both 10- and 20-gap crossings; they were in agreement (see figs. 3 and 4).

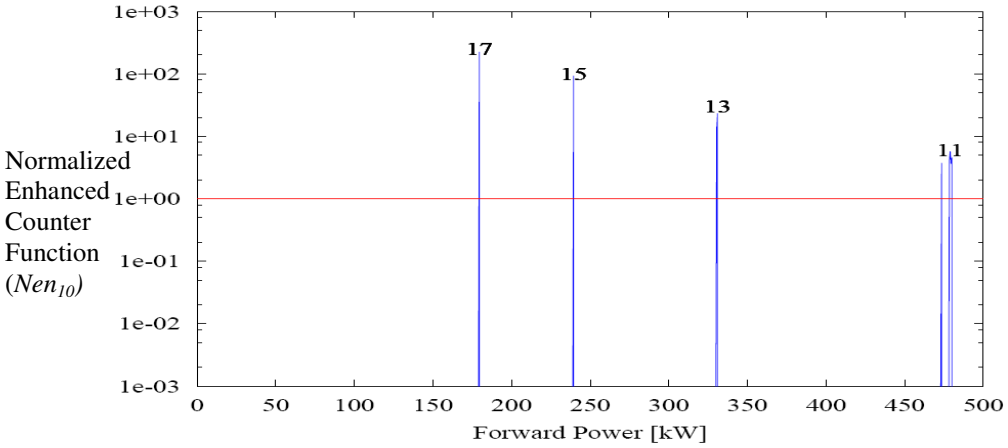

Fig. 3: The normalized enhanced counter function Nen_{20} for the TW mode. The Nen_{20} = 1 line is indicated [10].

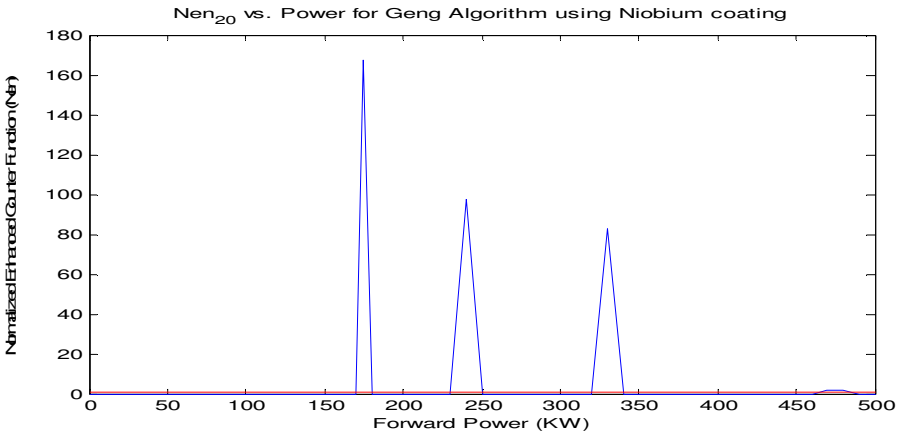

Fig. 4: The normalized enhanced counter function Nen_{20} for the TW mode. The Nen_{20} = 1 line is indicated.

IV. RESULTS AND DISCUSSION

Following the validation of the proposed MP algorithm, two simulation scenarios were implemented for 0 kW to 500 kW at 500 MHz operating frequency. The first (I) scenario involved the use of silver coating with the ***exclusion*** of reflected electrons; only true secondary electrons were assumed to be emitted from the metal surface. The second (II) scenario also involved the use of silver coating but

with the ***inclusion*** of reflected electrons, that is, in addition to the true secondary electrons, reflected inelastic and elastic electrons were also accounted for.

Table 1 shows the normalized enhanced counter function values (*Nen*) obtained for various simulation scenarios at a maximum of 10 electron-wall collision events. The *Nen* values in the second column are obtained after implementing the Geng algorithm on a niobium coating while those in the third column are obtained after implementing the same algorithm on a silver coating. The fourth column shows the values obtained after using a modified Geng algorithm which has incorporated reflected electrons into the Geng SEY model (eqn. 7) in order to analyze the MP characteristics of a silver coating. The shaded rows are *Nen* values which indicate possible MP initiations. **Bold** *italicized* values in the table represent extrapolated results.

Table 1 Normalized Enhanced counter function for certain values for power levels from 10 kW to 500 kW

MUT :	Niobium	Silver	Silver
ALGORITHM :	Geng	Geng	Modified Geng
SEY :	True sec (*Ts*) only	True sec (*Ts*) only	*Ts* plus Reflected
Power (kW)	***Nen***	***Nen***	***Nen***
0	0	0	0
10	0.008	0.048	0.057
-	-	-	-
110	0.014	0.006	0.008
120	0.742	0.406	1.441
-	-	-	-
330	1.59	4.724	2.854
-	-	-	-
420	1.018	***362.582***	***184.42***
-	-	-	-
500	0.458	0.368	0.647

Comparison of *Nen* Values for MP Initiating Transmit Power Levels

Fig. 5 shows a comparison of the normalized enhanced counter function values (*Nen*) for MP initiating power levels on simulation scenarios (I) and (II). Evaluation showed that the latter scenario, which took into consideration the reflected electrons, had 38% more transmit power levels with larger values of *Nen* than for the former scenario which did not take reflected electrons into consideration. The *Nen* values are determined by dividing the total number of generated secondary electrons by the initial number of primary electrons. It may be taken as the average number of secondary electrons generated by a single impacting electron. Thus, the conclusion in this comparison is that the simulation scenario that took into consideration reflected electrons generates more "secondaries" per impacting primary than the scenario that did not take reflected electrons into consideration.

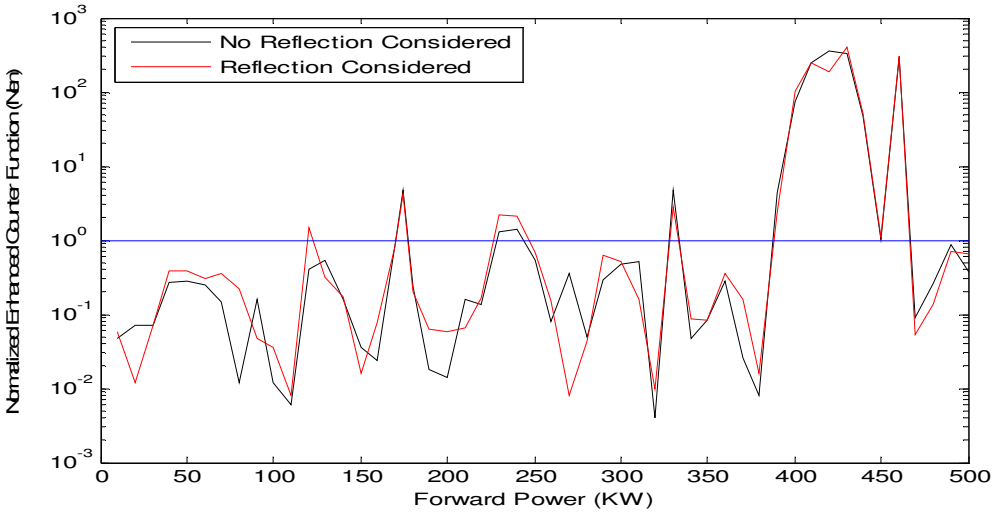

Fig. 5: Comparison of simulation scenarios (I) and (II)

It was also observed that, in addition to all the possible MP initiating power levels obtained from simulation scenario (I), one additional power level, 120 kW, also indicated the possibility of MP initiation in simulation scenario (II). The only explanation for this is that the reflected electrons which had not been considered in the first simulation scenario contributed to this MP initiation process. This shows that it is possible to overlook a subtle breakdown power (such as 120 kW in this case) if reflected electrons are not properly accounted for.

Modification Zones

The proposed algorithm provided a retrace functionality that tracks each emitted primary electron, including secondary electrons generated by the electron-wall impacts. The retrace functionality has the capability to monitor which primary and secondary electrons where sustained to the end of the entire multipacting process for any operating frequencies and transmit powers. Basically, the features included:

I. An Identification (ID) Management System which marks each primary electron with a unique identification code
II. A Parent-Child ID Management System which pairs off each child secondary electron with its parent primary electron.
III. A Parent-Child ID Management System which pairs off each child secondary electron with its parent secondary electron.
IV. A static link between the sustained primary electrons and their emission position and EM field data.

A retrace analysis of electrons (primary and corresponding secondary electrons) that survived the maximum electron-wall collision count was used to identify plausible zones (or points) of MP initiation. These zones represent locations on the rectangular waveguide that may need to be modified using any of the suppression techniques, such as surface modification (coating, sputtering, etc) or geometry modification (cutting, grooving, ridges, etc).

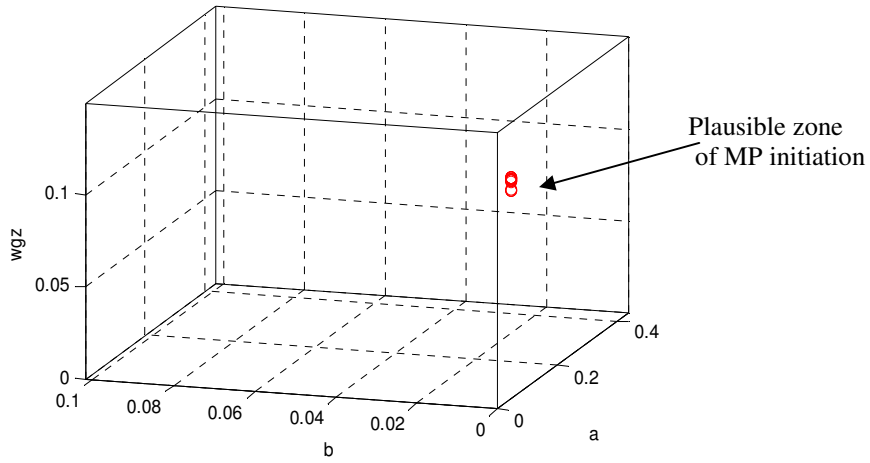

Fig. 6: Geometry modifiable zones

Fig. 6 shows a typical gridded rectangular waveguide with dimension a = 0.433 m, b = 0.102 m. The simulation scenario was done at a transmit power level of 120 kW. At the end of the 10^{th} iteration, a retrace of the electron dynamics indicated the plausible zones or (points) of MP initiation. Modification of this zone may likely lead to MP suppression. In contrast to the extensive modification approach currently adopted in the space industry (for the implementation of suppression features) which requires a complete coating or cutting of several grooves on the wall surface of rectangular waveguides, the proposed algorithm pinpoints the zones for the modifications, hence reducing the cost and time needed for the application of suppression features on space-bound rectangular waveguides.
The section may be summarized as follows:

1) The MP process analysis which took into consideration the reflected electrons had a higher percentage of breakdown power levels with larger values of normalized enhanced counter function than those which did not take reflected electrons into consideration. This means that MP analysis that excludes reflected electrons inadvertently under quantify the total amount of electrons present within a system.
2) It is crucial to account properly for reflected electrons during a multipacting process investigation in order to avoid overlooking subtle breakdown powers. This point is critical as it guarantees improved reliability of rectangular waveguides that are operated at multiple high power levels because component failure will not occur as a result of an unidentified MP initiating power.
3) It is possible to identify critical points of electron emission which can result to breakdown or system failure. This information can therefore be used to optimize the suppression procedures on the geometries of interest, hence reducing the manufacturing resource requirement for space-borne waveguides.

V. CONCLUSION

This work has presented a multipactor prediction algorithm for a rectangular waveguide geometry configured for a TE_{10} propagation mode which adequately accounted for reflection electrons in its design and implementation. The results obtained from the implemented algorithm underscored the possibility of inadvertently under-quantifying the total amount of electrons present within a system after collision events and also the likelihood of overlooking subtle multipactor breakdown powers where proper account is not given for reflected electrons during a multipacting process investigation.

ACKNOWLEDGEMENT

We acknowledge and appreciate the National Space Research and Development Agency (NASRDA), Nigeria, for providing the opportunity to engage in this research.

REFERENCES

[1] Geng R.L., Belomestnykh S., H. Padamsee, Goudket P., Dykes D.M., Carter R.G. (2004), *Studies of Electron Multipacting in CESR Type Rectangular Waveguide Couplers*, Proceedings of EPAC, pp. 1057-1059

[2] *Crossed-Field Amplifier with Multipactor Suppression* (2011), World Intellectual Property Organization (WIPO), http://www.wipo.int/pctdb/en/wo.jsp.

[3] Vicente C., Mattes M., Wolk D., Hartnagel H. L., Mosig J. R. and Raboso D. (2005), *FEST3D-A Simulation Tool for Multipactor Prediction*, *Proc. MULCOPIM 2005*, ESTEC-ESA, Noordwijk, The Netherlands, 2005, pp. 11-17.

[4] Becerra G. E. (2007), *Studies of Coaxial Multipactor in the Presence of a Magnetic Field*, U.S. Department of Energy Report, Plasma Science and Fusion, Vol. 99, pp 26-41.

[5] Seviour R. (2005), *The Role of Elastic and Inelastic Electron Reflected in Multipactor Discharges,* IEEE Transactions on Electron Devices, VOL. 52, NO. 8, AUGUST 2005 1927, pp. 1927-1930.

[6] Aviviere Telang, Antonio Panariello, M. Yu and R. Mansour (2011), *Multipactor Breakdown Simulation Code*, 7th International Workshop on Multipactor, Corona and Passive Intermodulation, MULCOPIM Valencia 2011

[7] José R. Montejo Garai, Carlos A. Leal, Jorge A. Ruiz Cruz, Jesús M. Rebollar Machaín, Teresa Estrada (2011), *Multipactor Prediction in Waveguide Band-Stop Filters with Wideband Spurious-free Response*, 7th International Workshop on Multipactor, Corona and Passive Intermodulation, MULCOPIM Valencia 2011

[8] Furman M. A. and Pivi M. T. F. (2003), *Simulation of Secondary Electron Emission Based on a Phenomenological Probabilistic Model*, Center for Beam Physics, Accelerator and Fusion Research Division, CA, USA, pp 1-31.

[9] Gusarova M.A, Kaminsky V.I., Kutsaev S.V., Lalayan M.V., Sobenin N.P., Kravchuk L.V., and Tarasov S.G. (2008), *Multipacting Simulation in RF Structures*, Proceedings of LINAC08, Victoria, BC, Canada, MOP082, pp. 265-267

[10] Geng R.L. and Padamsee H.S. (1999), *Exploring Multipacting Characteristics of a Rectangular Waveguide*, Proceedings of Particle Accelerator Conference, New York, NY., Vol. 05, pp. 429

[11] Juan L., Francisco P., Manuel A., Luis G., Isabel M., Elisa R. and David R. G. (2006), *Multipactor Prediction for On-Board Spacecraft RF Equipment with the MEST Software Tool*, IEEE Transactions on Plasma Science, Vol. 34, No. 2.

[12] Landau L.D and Lifshitz E.M (2000), Mechanics: Course of Theoretical physics, 3rd Ed., vol. 1, Butterworth and Heinemann Publication, pp. 41- 53

[13] Bellan P. M. (2004), *Fundamentals of Plasma Physics*, pp. 14-16

AUTHORS

AKOMA Henry E.C.A is a research engineer with the National Space Research and Development Agency (NASRDA), Abuja, Nigeria, and is currently engaged in his doctoral degree program at the University of Ilorin, Ilorin, Nigeria. He obtained a Master of Engineering (MEng) degree in Electrical Engineering (Communications Option) with Distinction from the Federal University of Technology, Minna, Nigeria. . He has published a book on the Fundamentals of Space Systems Engineering and has published several journal and conference papers particularly in the field of multipaction. Engr Akoma Henry E.C.A is a Registered Engineer, Council for the Regulation of Engineering in Nigeria (COREN). He is also a member of the Nigerian Society of Engineers (MNSE).

ADEDIRAN Yinusa Ademola is a professor of Electrical and Electronics Engineering presently is the head of Electrical and Electronics Engineering, Faculty of Engineering and Technology, University of Ilorin. He Obtained Doctor of Philosophy, Federal University of Technology, Minna, Nigeria, Master of Science (M.Sc.) in Industrial Engineering University of Ibadan and Master of Science (M.Sc.) in Electrical Engineering (Telecommunications Option) with Distinction, Technical University of Budapest, Hungary. He has published seven (7) books including Reliability Engineering, Telecommunications: Principles and Systems (First Edition), Fundamentals of Electric Circuits, Introduction to Engineering Economics, Applied Electricity, and Telecommunications: Principles and Systems (Second Edition) and Fundamentals of Electric Circuits. The

author has published over 70 journals, Conferences and manuscripts in Electrical & Electronics Engineering. Professor Yinusa Ademola Adediran is a Registered Engineer, Council for the Regulation of Engineering in Nigeria (COREN). He is a member of several professional society including Fellow, Nigerian Society of Engineers (FNSE),Member, Institute of Electrical & Electronic Engineers, USA (MIEEE), Corporate Member, Nigerian Institute of Management, Chartered (MNIM),Member, Quality Control Society of Nigeria (MQCSN).